RSC Chemical Biology

ROYAL SOCIETY OF CHEMISTRY

PAPER

View Article Online
View Journal | View Issue

Check for updates

Cite this: *RSC Chem. Biol.*, 2025, 6, 263

Protein stabilization in spray drying and solid-state storage by using a 'molecular lock' – exploiting bacterial adaptations for industrial applications†

Wiktoria Brytan, Tewfik Soulimane and Luis Padrela *

Small, stable biomedicines, like peptides and hormones, are already available on the market as spray dried formulations, however large biomolecules like antibodies and therapeutic enzymes continue to pose stability issues during the process. Stresses during solid-state formation are a barrier to formulation of large biotherapeutics as dry powders. Here, we explore an alternative avenue to protein stabilisation during the spray drying process, moving away from the use of excipients. In thermophilic proteins, the presence of C-termini extensions can add to their stability by increasing molecular rigidity. Hence, we explored a unique thermostable amino acid extension in the C-terminal of an aldehyde dehydrogenase tetramer originating from *Thermus thermophilus* HB27 (ALDH*Tt*), and its ability to stabilise the large enzyme against drying stresses. The presence of the C-terminal extension was found to act like a 'molecular lock' of the oligomeric state of the ALDH tetramer upon spray drying. Removal of the extension, mimicking the structure of mesophilic ALDHs, promoted the formation of aggregates and dissociative states. The ALDH protein with the 'molecular lock' retained ~24% more activity after spray drying and retained up to 16% more activity during solid state storage than its mutant. We proposed a mechanism for the protection of oligomeric proteins by the distinct C-terminal extension under stresses involved in solid formation. Additionally, the process of spray drying an excipient-free ALDH is achieved using a design of experiments approach, increasing its breadth of application in the biocatalysis of aldehydes.

Received 23rd August 2024,
Accepted 18th December 2024

DOI: 10.1039/d4cb00202d

rsc.li/rsc-chembio

Open Access Article. Published on 19 December 2024. Downloaded on 5/22/2026 1:24:05 PM.
This article is licensed under a Creative Commons Attribution-NonCommercial 3.0 Unported Licence.

1. Introduction

Formulation of proteins in the solid-state has grown in popularity due to its potential in product stabilisation, as well as offering new routes of administration for protein therapeutics such as oral and inhalable forms. The removal of water improves long-term protein stability by reducing mobility of protein molecules, impeding degradation pathways such as oxidation and hydrolysis and inducing conformational changes under raised temperature conditions.[1] Spray drying is a well-established method for producing protein and peptide powders with controlled particle properties, for a range of applications including production of dry powder inhalables (DPI) and continuous process implementation. Although the technique is popular for small, stable peptides, spray drying of large biomolecules with a quaternary assembly proves difficult. Currently, all FDA-approved spray dried biopharmaceuticals are peptides.[2] Thermal degradation in spray drying, along with the tendency of large amphiphilic proteins to adsorb onto air/liquid or solid/liquid interfaces, increases the likelihood of structure denaturation and protein–protein interaction. The phenomenon is intensified by the presence of mechanical stresses which exist during pumping of feed solutions or atomisation.[3] This can yield high volumes of aggregates through non-specific binding at the interface of atomised droplets.[4] Spray drying may also induce changes in the secondary structure of proteins by removal of the solvation shell and disruption of hydrogen bonding.[5] These issues are often tackled by addition of stabilisers to replace water molecules or preventing surface adsorption (*e.g.* sugars and surfactants) or by process optimisation (*e.g.* lowering outlet temperature, T_{out}, or lowering atomising gas flow rate).[3,6,7] Often, production of spray dried protein powders is a delicate balance between achieving dry, stable powders with little product degradation, and the formulation required. Excipients, such as surfactants and sugars, can pose issues at high concentrations during spray

SSPC – The Science Foundation Ireland Research Centre for Pharmaceuticals, Department of Chemical Sciences, Bernal Institute, University of Limerick, Limerick, Ireland. E-mail: Luis.Padrela@ul.ie

† Electronic supplementary information (ESI) available. See DOI: https://doi.org/10.1039/d4cb00202d

© 2025 The Author(s). Published by the Royal Society of Chemistry

Open Access Article. Published on 19 December 2024. Downloaded on 5/22/2026 1:24:05 PM. This article is licensed under a Creative Commons Attribution-NonCommercial 3.0 Unported Licence.

drying, due to increased stickiness of the powders.[8] Additionally, production of DPIs (Dry Powder Inhalables) requires careful selection and minimisation of excipients, due to variable effects on particle properties, such as density and particle size, as well as lung-related toxicity.[9] The path is therefore open for alternative stabilisation methods of spray-dried protein products.

Extensions of the C-termini in thermophilic proteins have been widely reported in the literature. Their presence is often correlated with increased thermostability and molecular rigidity. These structures may provide a stabilisation effect by increasing disulfide bridging[10] or increasing hydrogen bonding on the molecule surface.[11] In particular, helical C-terminal extensions have been showcased in increasing surface bonding in thermophilic, bacterial proteases and mutases.[12,13] Several proteins from the ancient bacterial species *Thermus thermophilus* have identifiable C-termini extensions that act as 'thermal clamps'.[11,14] One such extension can be identified in the aldehyde dehydrogenase (ALDH) protein expressed by the *Thermus* phylum. Our previous work takes a deeper look at the function and structure of the C-terminal extension of an ALDH natively expressed by *Thermus thermophilus*, strain HB27, referred hitherto as ALDH*Tt* (PDB entry: 6FJX).[15,16] ALDH*Tt* (Fig. 1) is a multifunctional enzyme capable of utilising both NAD and NAD(P) as an electron acceptor for the oxidation of a range of aldehydes and esters. ALDH proteins are widely studied in eukaryotic systems due to their role in the metastasis of various cancers, with overexpression of the protein causing cell proliferation and resistance to chemotherapies.[17] Prokaryotic ALDHs have also been recognised for their application in biocatalysis of toxic aldehydes, particularly in the removal of acetaldehyde during food processing.[18,19] ALDH*Tt* is homotetrameric in nature, with each monomer weighing 59 kDa and a sequence length of 530 amino acids. In a previous study we have identified the role of the C-terminus by creation of a mutant of ALDH*Tt* which was truncated by 22 amino acids effectively removing the C-terminus (ALDH*Tt*-508),[16] mimicking the length of mesophilic ALDH proteins. We showed that the C-terminal extension protects the protein from high-order aggregation, by measuring the hydrodynamic diameter under increasing temperature conditions using dynamic light scattering (DLS). The C-terminus was also responsible for the substrate specificity of ALDH*Tt*, limiting its affinity towards larger *ortho*-substituted aldehydes. Additionally, the positioning of the C-terminal extension over the substrate access tunnel of the enzyme limited its kinetic activity in solution, by blocking access to the catalytic cysteine. The C-terminus terminates in an α-helix, visible in the ribbon model in Fig. 1.

C-Terminal extensions that act as 'thermal clamps' or 'molecular locks' have not yet been explored for their applications in process development or protein stabilisation applications. In this work, we describe the effect of a helical C-terminal extension on the activity, oligomeric stability and secondary structure conformation of an aldehyde dehydrogenase protein during the spray drying process. The work aims to explore the C-terminus extension in depth for its application in the stabilisation of large, multi-subunit proteins during spray drying.

To the best of our knowledge, there is no existing comparative study on the effect of a mutation on protein solid-state stability. This work aims to fill the gap on the stabilisation of protein spray-dried formulations using structural modifications. Rationally, mutant industrial enzymes are routinely spray dried,[20] surprisingly however we cannot identify a study which delves into the detailed effect of a mutation on the spray drying stability of a protein and therefore this work adds to our knowledge of production of solid-state enzymes for biocatalysis applications.

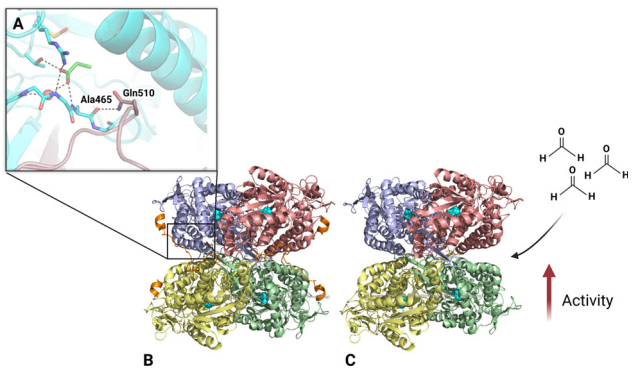

Fig. 1 The relationship between the substrate tunnel and C-terminal extension in ALDHTt-native (A), ALDHTt-native (B) and ALDHTt-508 (C) tetrameric structure as a ribbon model. The C-terminal extension is shown in orange while the catalytic residue CYS295 is shown in ball-and-stick model within each monomer (cyan). The figure was modelled using PyMOL 2.5. (A) was adapted from ref. 15.

2. Experimental

2.1 Production of ALDH*Tt*-native and ALDH*Tt*-508

The two proteins were recombinantly expressed in *E. coli* BL21 (DE3) cells as described previously.[13] Protein solutions of >85% purity were achieved by Nickel affinity purification of the His-tagged proteins, with an addition of a 5 or 15-min heat treatment step for ALDH*Tt*-508 and ALDH*Tt*-native, respectively. The purification buffer, which consisted of 20 mM Tris–HCl, 5 mM β-mercaptoethanol, 10 mM imidazole and 200 mM NaCl at pH 7.5, was dialysed overnight against water, and the protein was flash-frozen and stored at −80 °C. Purity of batches was confirmed by SDS-PAGE and SE-HPLC. The concentration of the ALDH protein was measured at 280 nm, using a NanoDrop Spectrophotomer (Model 1000, ThermoFischer Scientific) with an extinction coefficient (ε) of 1671 M^{-1} cm^{-1}, prior to spray drying.

2.1.1 Sodium dodecyl sulfate polyacrylamide gel electrophoresis (SDS-PAGE). A 4–15% mini-PROTEAN TGX gel (BioRad) was used to confirm purity of protein batches. Each protein sample was diluted in a reducing buffer consisting of 0.0635 M Tris, 2% SDS, 10% glycerol and 5% 2-mercaptoethanol, with 0.01% bromophenol blue for band visualisation. The samples were denatured at 95 °C for

© 2025 The Author(s). Published by the Royal Society of Chemistry

Open Access Article. Published on 19 December 2024. Downloaded on 5/22/2026 1:24:05 PM. This article is licensed under a Creative Commons Attribution-NonCommercial 3.0 Unported Licence.

10 minutes and applied to the gel along with a protein ladder (10–180 kDa) for molecular weight estimation. The electrophoresis was run at 120 V for 10 minutes, followed by 230 V for 20 minutes. The running buffer consisted of 25 mM Tris, 0.2 M glycine and 0.1% SDS. The gels were stained using Coomassie Instant Blue stain (Abcam) for 1 hour, then destained using Deionised water. Protein molecular weight was determined by comparing visualised bands to a molecular weight marker, PageRuler™ Prestained Protein Ladder, 10 to 180 kDa which was obtained from ThermoFisher Scientific.

2.2 Formulation of feed solutions

For spray drying (SD) of both ALDH*Tt* variants, protein solutions were made up in deionised water to a 0.1% (w/v) solids content. No further excipients were added to the formulations.

2.3 Spray drying (SD)

A 2-factor, 2-level Box-Behnken design of experiments (DoE) with a centre point (Table 1) was used to evaluate the effect of outlet temperature (T_{out}) and feed flow rate (FFR) on the particle size, moisture content, activity and oligomeric stability of ALDH*Tt*-native and ALDH*Tt*-508 (ALDH*Tt* with excised C-terminal extension). Spray drying (SD) of both proteins was performed using a Büchi B-290 Mini Spray Dryer (Büchi Labortechnik AG, Flawil, Switzerland). JMP Pro 17.0 software was used for the design and evaluation of the DoE. The outlet temperature limits were decided by taking into consideration the melting point of ALDH*Tt* ≈ 84 °C.[15] T_{out} is routinely selected as a critical parameter in protein spray drying, in terms of product quality and stability and therefore was deemed a necessary factor in this study.[21] FFR has an impact on droplet formation and final particle size, affecting product outputs such as aggregation and moisture content.[22]

An external mixing, two-fluid nozzle of ∅ 0.7 mm inner diameter and ∅ 1.4 mm nozzle cap was used to spray the protein feeds. Air was used as the atomising gas and the system was operated in open loop mode during drying. The atomising gas flow rate was kept constant at 1374 L h^{-1}. The aspirator was operated at (35 m^3). The spray dried powders collected were stored at −20 °C with silica beads for further analysis. Inlet temperatures can be found in the ESI† (Table S1).

2.3.1 Morphology and particle size analysis. Particle size and morphology were analysed using a Hitachi SU-70 scanning electron microscope (SEM). Samples stored at −20 °C were fixated on carbon tape on aluminium stubs suitable for the SEM. The samples were sputtered with gold, under vacuum, using a EmiTech K550 coating unit. The accelerating voltage of the electron beam was set to 10 kVA or 5 kVa for all samples. The particle size of 200 particles from at least three different images (per sample) was measured manually.

Table 1 Upper (+), lower (−) limits and centre point for the input factors considered in the 2-level Box-Behnken DoE

Input factors	+	−	Centre
FFR (ml min^{-1})	4	1.5	2.75
T_{out} (°C)	100	70	85

2.3.2 Karl–Fischer titration. Samples stored in the desiccator were analysed for residual moisture content using volumetric titration using the Hanna HI903 Karl Fischer automatic titrator (Hanna Instruments) in Week 0. A 1 mg ml^{-1} water standard (Aqualine, Fisher Chemical) was used for standardisation of the reagents.[23] Approximately 15 mg of each sample was back-weighed and inserted into the methanol-based solvent through a septum cap. The sample was titrated against methanol-free HYDRANAL™ – Composite 1 reagent (Honeywell).

2.3.3 NAD-coupled enzymatic activity assay. The enzyme assays for both ALDH*Tt*-native and ALDH*Tt*-508 were conducted as described elsewhere.[15,16] The enzymatic reaction consisted of 60 nM ALDH, 0.4 mM NAD+ (nicotinamide adenine diphosphate sodium salt, Sigma Aldrich) and 1 mM of the substrate hexanal (Sigma Aldrich). All solutions were prepared in 10 mM potassium phosphate buffer (pH 8.0) to a volume of 1 ml. Powdered ALDH samples were reconstituted in the buffer and adjusted to 60 nM. The components were warmed to 50 °C in a water bath directly prior to analysis. An Evolution 201 Series UV-vs spectrophotometer (ThermoFisher) was used to conduct the analysis. The production of NADH at λ = 340 nm was measured at every 5 s for 120 s. All assays were performed in triplicate. The enzyme activity was calculated by the change in NADH concentration in the solution per minute and expressed in 1 U mg^{-1} (Specific Enzyme units) of ALDH, which was equal to 1 μmol min^{-1} of NADH. Analysis of enzymatic activity was performed within 24 h of spray drying. Residual activity was calculated as follows:

$$\frac{m_1}{m_2} \times 100$$

where m_1 is the average slope of the rise in absorbance (at 340 nm) *versus* time for the protein before SD, and m_2 is the average slope for the protein sample after SD (weeks 0, 2, 4, 8 or 12).

2.3.4 Size exclusion high performance liquid chromatography (SE-HPLC). A SE-HPLC column (AdvanceBio SEC 300 Å, 2.7 μm, 8 × 300 mm, Agilent Technologies) coupled to a 1260 Infinity HPLC system (Agilent Technologies) was used for the detection and quantification of soluble aggregates and dissociation of the quaternary structure of ALDH*Tt*. A 10 mM Potassium phosphate buffer, pH 8.0 was used as the mobile phase. The samples were reconstituted where possible, centrifuged at 10 000 rpm for 10 minutes to remove insoluble particulates and adjusted to 0.5 mg ml^{-1}. Approximately 50 μl of each sample was injected onto an equilibrated column at a flow rate of 1 ml min^{-1}. The detector was set to 220/280 nm. The column was calibrated using a protein mixture of Thyroglobulin bovine MW ∼ 670 000 Da, γ-globulins from bovine blood MW ∼ 150 000 Da, Ovalbumin MW ∼ 44 300 Da and Ribonuclease A type I-A MW ∼ 13 700 Da.

2.3.5 Turbidimetry. Nephelometric measurements were taken to evaluate the level of insoluble particulates in

Open Access Article. Published on 19 December 2024. Downloaded on 5/22/2026 1:24:05 PM. This article is licensed under a Creative Commons Attribution-NonCommercial 3.0 Unported Licence.

reconstituted powder samples. A Hach Lange 2100Q portable Turbidimeter was used. Samples of 0.025 mg ml^{-1} were prepared in 15 ml of distilled water and briefly inverted before analysis. Samples were measured by 90° light scattering at 860 nm. Unprocessed ALDH*Tt*-native and ALDH*Tt*-508 were used as controls.

2.3.6 Solid-state attenuated total reflectance-Fourier transform infrared spectroscopy (ss-ATR-FTIR). Interferograms of ALDH*Tt*-native and ALDH*Tt*-508 were obtained using a Nicolet iS50 FTIR Spectrometer (Thermo Fisher Scientific) in solid state. Spectra were recorded from 4000 cm^{-1} to 600 cm^{-1} with a resolution of 2 cm^{-1}. Thermally treated powder samples were analysed by heating the samples at 120 °C for 2 h and used as a control. Spectra were analysed using Prism software (ver. 8.0.1), where the second derivative was taken of each spectrum and maximum–minimum normalised. The spectra were allowed 20-point Savitzky–Golay smoothing.

2.3.7 Circular dichroism (CD). The secondary structure spectra of the ALDH*Tt* samples were analysed using a Chirascan Plus CD spectrophotometer (Applied PhotoPhysics Ltd, UK). The spectra were recorded in the Far-UV wavelength range of 180–250 nm. The path length was 1 cm, and a wavelength step of 1 nm. Wavelength scans were obtained in triplicate of protein solutions of 5 μg ml^{-1} in 10 mM potassium phosphate buffer, pH 8.0. The spectra were averaged, background corrected using the blank and allowed 6-point Savitsky–Golay smoothing for graphing purposes. For spectral deconvolution, raw spectra was analysed using was the (Beta Structure Selection) BestSel algorithm (**https://bestsel.elte.hu**).

2.4 Statistical analysis

Statistical analysis (Standard least square model or Student's *t*-test) was performed using JMP Pro 17.0. The results are presented as mean ± standard deviation, unless otherwise stated. Influences of the variable on the response were deemed to be significant at a level of $p < 0.05$ (*). Levels of significance were annotated as $p < 0.05$ (*), $p < 0.005$ (**), $p < 0.0005$ (***) and $p > 0.05$ (ns).

3. Results and discussion

3.1 Spray drying of ALDH*Tt*: process considerations

By applying the Box–Behnken DoE, a uniform, active and excipient-free powder of aldehyde dehydrogenase with and without the C-terminal extension was produced using the Büchi B-290 Mini Spray Dryer. Spray drying (SD) of both macromolecules showed no significant changes in the integrity of the primary structure compared to an untreated protein reference, visualised by SDS gels. The theoretical tetrameric size of ALDH*Tt*-native and ALDH*Tt*-508 was determined as 237.5 kDa and 228.3 kDa, with each monomer possessing a molecular weight of 59.4 kDa and 57.1 kDa, respectively. The results of the SDS-PAGE can be viewed in Fig. S1 (ESI†). Karl-Fisher titration indicated the protein powders possessed a residual moisture content (RM) of 5–12%, leaving the molecules in a fully flexible state (Fig. 1B). To achieve a rigid conformation, complete removal of the protein's hydration layer is necessary, corresponding by achieving between 0.04–0.07 mg H_2O per mg protein.[24,25] Considering this, a 0.4–0.7% RM would be necessary to limit the motor and function of excipient-free ALDH*Tt* powders. Statistical analyses showed that the feed flow rate (FFR) was positively correlated with RM, and outlet temperature (T_{out}) showing little to no impact on water contents of the enzyme powders (Fig. S2, ESI†). Using the lowest FFR and highest T_{out} parameters of the DoE we were able to achieve an RM% within the typical ranges reported for the Büchi B-290 Mini spray drying system[26,27] however without the presence of bulking agents, sugars or polymers, the energy necessary to sufficiently dry atomised droplets is high. Considering the mobility of macromolecules and a lack of vitrification matrix usually provided by the use of excipients the storage stability of these powders was expected to be low, with increased intermolecular interactions at room temperature.[28]

The major advantage of spray drying over other methods is the ease of particle engineering of resulting powders. Formulation of excipient-free protein powders resulted in particles of a collapsed and spherical morphology as viewed by scanning electron microscopy (SEM) (Fig. 2a). Exhibited morphology did not change for ALDH*Tt*-native and ALDH*Tt*-508 (Fig. S3 and S4, ESI†). Particle size was also unaffected by the removal of the C-terminal extension, with no significant difference between the particle size median values of the two ALDH*Tt* powders ($p = 0.9$, ns) (Table S2, ESI†). These results signify that the molecular mutation does not impact process capabilities in spray drying. Additionally, the distribution width (*i.e.* span) of all powders was lower than 1.1, representing a narrow particle size distribution (Table S2, ESI†).

Statistical analyses of the particle size data revealed outlet temperature as a defining factor of the pure-protein system (*p*-value ≤ 0.0005 (***)) negating the effect of feed flow rate (Fig. S2A, ESI†). The diffusivity of globular macromolecules through aqueous medium decreases with molecule size and system temperature according to the Einstein–Smoluchowski equation.[29] Where D is the diffusion coefficient, k_B is the Boltzmann's constant, T is the absolute temperature and ξ is the friction coefficient considering a spherical particle of radius 5.72 nm (ALDH*Tt*-native) and 5.57 nm (ALDH*Tt*-508).[16]

$$D = \frac{k_B T}{\xi}$$

assuming temperature of the water droplet as T_{out}, the diffusion coefficient of ALDH*Tt*-native and ALDH*Tt*-508 was calculated as 1.67×10^{-10} and 1.72×10^{-10} m^2 s^{-1} respectively, (T_{out} = 100 °C) and 1.09×10^{-10} and 1.11×10^{-10} respectively (T_{out} = 70 °C). Without excipients the diffusion of solids in the atomised droplet can be entirely attributed to the movement of the protein molecules. Lower temperatures at T_{out} result in lower diffusivity, leading to more severe particle collapse. Since the particles presented in Fig. S3 and S4 (ESI†) assume a collapsed, wrinkled morphology, their size is dictated by the rate of evaporation from the inside of the particle and the

© 2025 The Author(s). Published by the Royal Society of Chemistry

Open Access Article. Published on 19 December 2024. Downloaded on 5/22/2026 1:24:05 PM. This article is licensed under a Creative Commons Attribution-NonCommercial 3.0 Unported Licence.

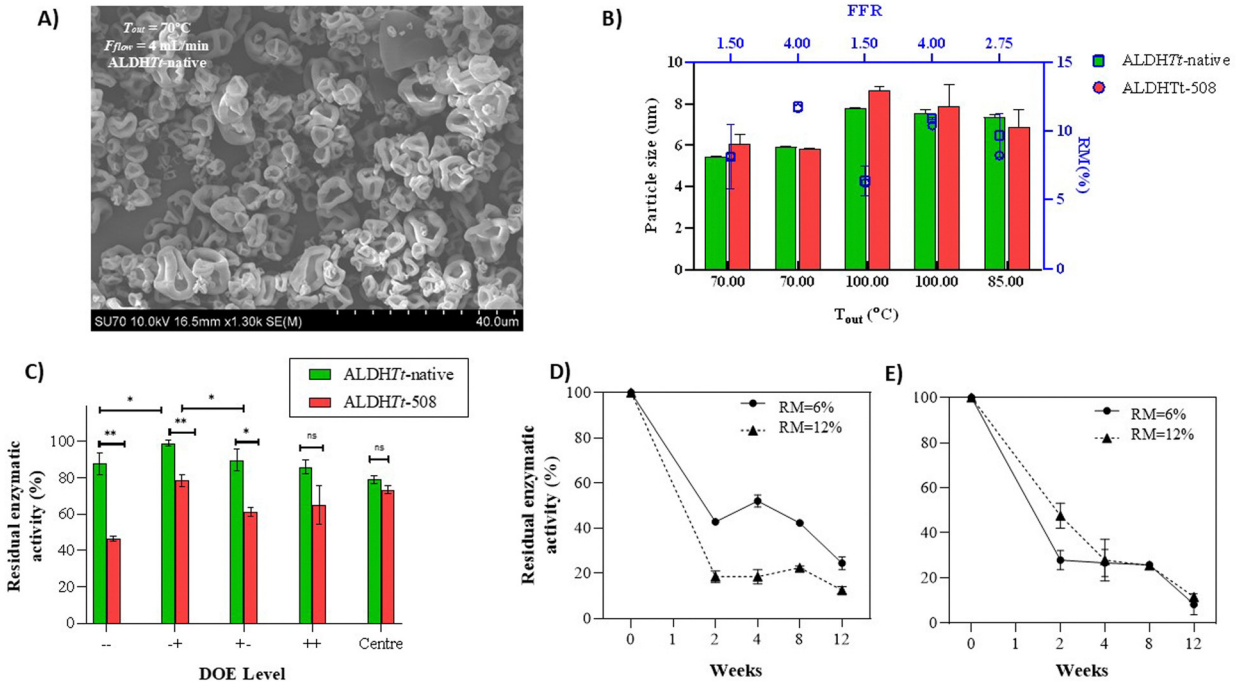

Fig. 2 (A) Morphology of ALDH*Tt*-native particles viewed with scanning electron microscopy (SEM). (B) Effect of feed flow rate (FFR) and outlet temperature (T_{out}) on the moisture content and particle size of ALDH*Tt*-native and ALDHTt-508. (C) Residual enzymatic activity of ALDH*Tt*-native (green) and ALDH*Tt*-508 (red) after spray drying (SD) (week 0) using process conditions of the DoE outlined in Table 1. (D) Residual enzymatic activity of ALDH*Tt*-native and (E) ALDH*Tt*-508 powders, spray-dried under process conditions of DoE level − +, (RM = 6%) and level + −, (RM = 12%) tested over a 12-week period at room temperature.

collapse of the solid crust at T_{out}. Temperature is hence a defining predictor of particle size and morphology in pure protein systems as opposed to mixtures.[30] For further analysis of the effect of the 'molecular lock' on the behaviour of ALDH*Tt* during spray drying, the driest (RM% = 6.4 ± 1.5, DoE level + −) and wettest (RM% = 11.8 ± 0.2, DoE level − +) powders were considered.

3.2 Implication of the 'molecular lock' on stability of ALDH*Tt* enzymatic activity and oligomeric stability during spray drying

The relationship between quaternary structure in large proteins and their activity is integrally linked. Although most multi-subunit proteins exist in many states in aqueous solutions and are capable of refolding to their functional state, issues arise during solid-state formation as the removal of water impedes the refolding of active forms.[7,31] A NAD-coupled enzyme assay and size-exclusion HPLC was used to determine impact of high energy spray drying on the stability and integrity of the ALDH tetramer, with and without the presence of a 'molecular lock' supporting the quaternary structure (methodology described in Section 2.4). ALDH*Tt*-508 exhibited a routinely higher specific enzyme activity (0.564 ± 0.12 U mg^{-1}) than ALDH*Tt*-native (0.432 ± 0.035 U mg^{-1}) prior to spray drying (SD). This behaviour was accredited to the loss of the C-terminal extension and thus open conformation of the active site to the substrate.[15,16] The oxidoreductase activity of ALDH*Tt*-508 is however diminished to a larger extent than ALDH*Tt*-native during the SD process. Considering the driest and wettest conditions of the process, ALDH*Tt*-508 retained up to 78.43 ± 5.72% activity and 61.17 ± 4.22% respectively, while ALDH*Tt*-native retained 98.9 ± 2.9% and 89.7 ± 10.0% oxidoreductase activity for the same DoE levels, respectively (Fig. 2C). The existing thermostability data of ALDH*Tt*-508 depicts only a 4 °C difference in the T_m of the tetramer (T_m = 80 °C) and no difference in the optimal temperature for catalysis of aldehydes between the native protein and ALDH*Tt*-508.[15,16] Temperature, however, is not the only degradative stress present in the SD method. Interfacial binding of the proteins to the air–water and solid–air interfaces promotes intermolecular interactions by grouping the molecules at the interface. Paired with shear forces present at the nozzle, which can expose aggregation-prone regions, interfacial stress may often be more detrimental to protein stability during SD than thermal events.[9,32] In a previous study, we established that the C-terminal extension acts as a 'molecular lock' for the ALDH*Tt* structure, and its removal increases rates of aggregation during heating, despite its small difference in T_m.[16] Removal of this molecular lock promotes interactions between previously buried hydrophobic regions in solution and is therefore likely to increase intermolecular binding at the droplet interface during spray drying. To assess whether loss of enzymatic activity was an effect of formed aggregates, powders were resuspended and injected onto a calibrated SE-HPLC column. ALDH*Tt*-native and ALDH*Tt*-508 both eluted as a tetramer, at 5.43 min and 5.59 min respectively, corresponding to a MW of 266.1 kDa and 239.49 kDa (Fig. 3A). ALDH*Tt*-native retained ~6–9% more

Open Access Article. Published on 19 December 2024. Downloaded on 5/22/2026 1:24:05 PM.
This article is licensed under a Creative Commons Attribution-NonCommercial 3.0 Unported Licence.

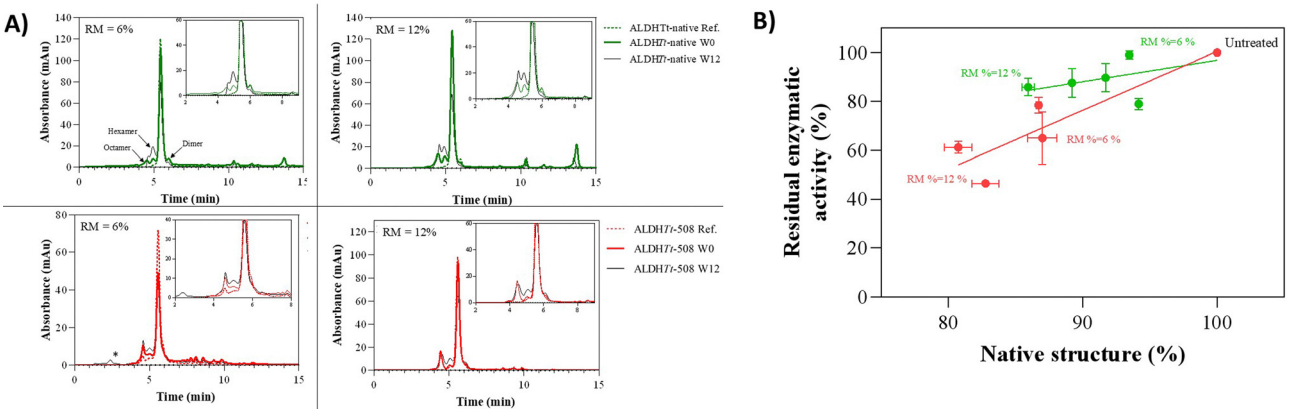

Fig. 3 (A) Size-exclusion high performance chromatography (SE-HPLC) elution profiles of ALDH*Tt*-native (top) and ALDH*Tt*-508 (bottom) untreated (Ref.) and reconstituted samples, at 280 nm wavelength detection. Aggregates of over 2 μm are indicated by an asterisk (*). (B) The relationship between percentage of residual enzymatic activity and percentage of native structure retained in spray dried powders of ALDH*Tt*-native (green) and ALDH*Tt*-508 (red).

of the native quaternary structure than ALDH*Tt*-508 (Table 2). Powders with a lower RM% and harsher processing conditions, lead to a higher rate of aggregation for both proteins, with up to 13.34% aggregate peaks detected for protein ALDH*Tt*-508 at Week 0 (W0), and 8.8% for ALDH*Tt*-native (Table 2). Similarly, harsher conditions led to higher rates of activity loss (Fig. 2C). The Pearson's correlation coefficient was calculated for the relationship between percentage of residual enzymatic activity and percentage of native structure retained by ALDH*Tt*-native and ALDH*Tt*-508 (Fig. 3B). These were found to be moderately positively correlated for ALDH*Tt*-native, $r(5) = 0.52$, $p > 0.05$ and strongly correlated for ALDHTt-508, $r(5) = 0.89$, $p = 0.04$. The high p-values for both proteins are due to the small sample size used in this study. These results suggest that the loss of enzymatic activity is at least partially due to the destabilisation of the active tetramer, as the percentage of residual activity is positively correlated to the percentage of tetramer retained. The presence of the 'molecular lock' improves SD stability of ALDH*Tt*, likely by preventing intermolecular interactions and dissociation once shear and thermal stresses are applied.

Dissociation of the tetrameric structure is present in both protein controls (prior to SD) (Table 2), and while it does not impede the protein's activity in aqueous conditions, the inability of dissociated states to reform after the SD process may lower the overall activity and exaggerate the presence of high molecular weight species. Presence of the 'molecular lock' in ALDH*Tt*-native lowers the presence of dissociative states in the powders at Week 0 (W0) and Week 12 (W12) (Table 2). The most prevalent aggregate peak in SE-HPLC corresponded to the theoretical MW of the protein hexamer (~360 kDa) and was present in both protein powders at Week 0. This peak was also present to a small extent in the untreatedALDH*Tt*-508 protein reference (Ref.) (Fig. 3A). This leads to the conclusion that dimers of ALDH*Tt* are involved in aggregate formation during SD and are incapable of refolding to the native tetramer after reconstitution. Stabilisation of the tetramer using the 'molecular lock' prior to SD improved the retention of the active oligomer during the process by preventing dissociation during stress. Additionally, dissociative states of ALDH*Tt* formed during the SD process are involved in aggregation during storage, suggested by the dip in levels of dissociative states after 12 weeks, and the increase in the hexameric peak in SE-HPLC chromatograms (Table 2 and Fig. 3A). During long-term storage of the solid-state enzymes, the oxidoreductase activity

Table 2 Calculated values of native structure, aggregates and dissociation present in ALDH*Tt*-native and ALDH*Tt*-508 spray dried powders

		ALDH*Tt*-native		ALDH*Tt*-508	
Powder RM (%)		12	6	12	6
Ref.	Native structure (%)	98.0 ± 0.0	98.0 ± 0.0	96.4 ± 0.1	100 ± 0.0[a]
	Aggregates (%)	0.0	0.0	2.3 ± 0.1	0.0
	Dissociation (%)	2.0 ± 0.0	2.0 ± 0.0	1.2 ± 0.0	0
W0	Native structure (%)	94.4 ± 1.1	91.5 ± 0.4	85.6 ± 0.3	85.1 ± 1.4
	Aggregates (%)	1.7 ± 0.1	8.8 ± 0.3	8.0 ± 0.2	13.3 ± 1.8
	Dissociation (%)	3.0 ± 0.7	0	6.4 ± 0.1	1.5 ± 0.3
W12	Native structure (%)	86.2 ± 0.0	79.7 ± 2.2	82.0 ± 7.4[b]	73.7 ± 0.7
	Aggregates (%)	11.7 ± 0.1	18.2 ± 2.2	14.1 ± 5.8	22.2 ± 0.4
	Dissociation (%)	2.1 ± 0.0	2.1 ± 0.1	3.9 ± 1.6	4.1 ± 0.3

[a] As detectable by the HPLC method. [b] Poor peak resolution due to aggregate formation.

© 2025 The Author(s). Published by the Royal Society of Chemistry

Open Access Article. Published on 19 December 2024. Downloaded on 5/22/2026 1:24:05 PM. This article is licensed under a Creative Commons Attribution-NonCommercial 3.0 Unported Licence.

decreased dramatically, and aggregates were formed, regardless of the powder RM% (Fig. 2D and E). Generally, proteins are stabilised in solid-state by the kinetic interactions between protein and excipient molecules, thus the stability of pure ALDH*Tt* powders was expected to be low at room temperature.[33] The lack of excipients in this work allowed us to observe the effect of the C-terminal extension or 'molecular lock' on storage stability. Indeed, the ALDH*Tt*-native with an oligomeric lock, showed better storage stability and integrity of the tetramer over 12 weeks (Fig. 2D, E and Table 2). Storage-related instability of proteins can be the outcome of various processes, including oxidation, denaturation at the solid interface and aggregation (covalent and non-covalent).[34] The severing of salt bridges of ALDH*Tt* upon removal of the C-terminus exposes aggregation-prone, hydrophobic regions. This is coupled with the increased flexibility of the molecules by exposure of the hydrophilic core, leading to increased mobility in a semi-aqueous environment (RM% = 6–12%). The loss of activity is therefore likely to be a result of a combination of denaturation of the structure and subsequent non-covalent aggregation detected in SE-HPLC (Table 2 and Fig. 3A). Given that the C-terminal extension, or 'molecular lock', slows down the rate of dissociation, and therefore decreases the chance of misfolding, ALDH*Tt*-native shows ~20% lower levels of aggregation than ALDH*Tt*-508 after 12 weeks at room temperature, and retains a proportionally similar level of activity (~16%). It is important to note, that although the 'molecular lock' protects against SD stresses and decreases initial levels of aggregation in the powders (at W0), the structure does not affect the rate at which aggregation occurs during storage. Thus, native ALDH*Tt* is protected to some extent at solid-state storage, by the induced rigidity of the C-terminal molecular lock prior to the drying process. SE-HPLC deals only with soluble aggregation, and any protein precipitates were excluded from analysis by centrifugation. This is particularly important for the quantification of ALDH*Tt*-508 aggregates which have been shown to exceed their solubility faster than aggregates of ALDH*Tt*-native.[16] Turbidimetry assays support the finding that ALDH*Tt*-508 powders are more prone to formation of precipitates than ALDH*Tt*-native, regardless of the SD conditions used. These results are presented in Table S3 (ESI†).

3.3 Implication of the 'molecular lock' on stability of ALDH*Tt* conformational analysis

Secondary structure conformational changes during SD and storage are commonly reported and are often a prerequisite to aggregate formation. When the C-terminal extension is removed from ALDH*Tt*-native, the mutation (1) removes the terminal α-helix capping the substrate access tunnel, (2) exposes hydrophilic side chains present in the largely α-helical catalytic domain, and (3) exposes the oligomerisation domain comprising of distinct β-sheets, from which it extends. Additionally, severing the bonds between the C-terminal tail and the oligomerisation domain of the opposing monomer causes loss of the strong salt bridge interactions present on the surface of the protein (secondary structure visualisation was achieved using multiple sequence alignment and homology modelling with **https://predictprotein.org**, sequence obtained from PDB; accession numbers 6FKV, 6FJX[15,35]).

Both proteins showed characteristic CD and ss-FTIR spectra of protein consisting of β-sheets and α-helices (Fig. 4). Deconvolution of the CD spectra was achieved using BestSel (**https://bestsel.elte.hu**) (Table S4 and Fig. 5, ESI†).

In its rehydrated state, ALDH*Tt*-native with 'molecular lock' showed little conformational change after spray drying. In Fig. 4A, ALDH*Tt*-native shows no major relaxation of the 208 and 222 nm native helical minima in either of the 'wet' or 'dry powders tested. Deconvolution of the CD spectra of ALDH*Tt*-native shows delicate changes in composition, including gains of anti-parallel B-sheets and loss of native helix. In general, ALDH*Tt*-508 lost more of its native structure after SD than ALDH*Tt*-native. One major difference was the gain of distorted helical structures in rehydrated samples (Table S4 and Fig. 5, ESI†). distinction between the helical backbone and the spectrally unique ends of the helix, where decreasing ratio of backbone to ends can be correlated to decreasing helical length.

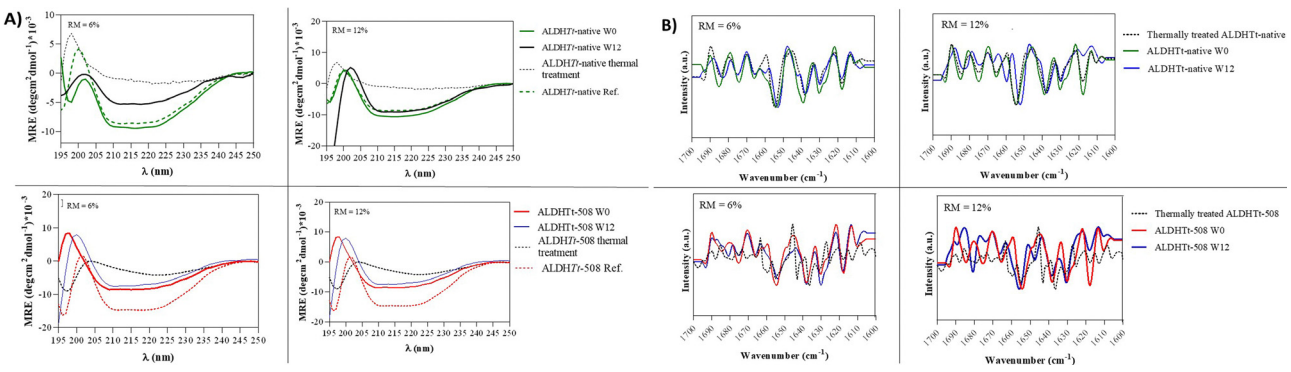

Fig. 4 (A) Circular dichroism (CD) spectra of 5 μg ml^{-1} ALDH*Tt*-native (top) and ALDH*Tt*-508 (bottom) directly after spray drying (W0) and after 12 weeks of storage (W12), compared to untreated reference (Ref.) and thermally treated samples. (B) Attenuated total reflectance-Fourier transform infrared (ATR-FTIR) spectra of spray dried powders of ALDH*Tt*-native (top) and ALDH*Tt*-508 (bottom) at week 0 (W0) and week 12 (W12). The spectra were compared to a thermally treated powder of each protein.

Open Access Article. Published on 19 December 2024. Downloaded on 5/22/2026 1:24:05 PM.
This article is licensed under a Creative Commons Attribution-NonCommercial 3.0 Unported Licence.

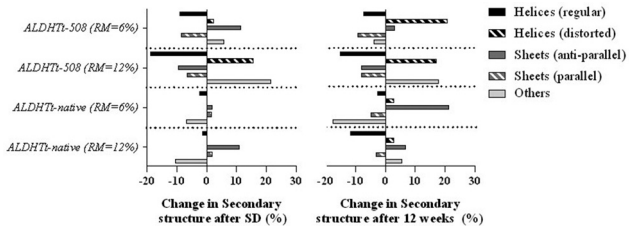

Fig. 5 Changes in secondary structure composition of ALDH*Tt*-native and ALDH*Tt*-508 after spray drying and after solid state storage for 12 weeks. Residual moisture contents of powders are indicated by RM%.

Spray drying and storage of ALDH*Tt*-508 powders decreases helical length and contributes to partial unfolding of the sensitive helical structure. Thermal treatment leads to complete loss of the helix, as demonstrated with other proteins (Table S4, ESI†).[36] Additionally, presence of the 'molecular lock' increases the formation of anti-parallel sheets under spray-drying stresses, suggesting an organized mechanism of aggregation.[37] In contrast, without the molecular lock, ALDH*Tt*-508 increases in 'disordered structures' or 'other' structures after spray drying (Fig. 5).

Deconvolution of solid-state Attenuated total reflectance-Fourier transform infrared (ss-ATR-FTIR) spectra, showed a major peak at 1655 cm^{-1} corresponding to α-helices (Fig. 4B). Two other major peaks were detected at 1632 cm^{-1} and 1638 cm^{-1} for both proteins, which were assigned to β-sheet structures. Less prominent peaks at 1663 cm^{-1} and 1675 cm^{-1} were assigned to 3^{10}-helices and turns, respectively. Thermally treated spectra of ALDH*Tt*-native are comparable with the enzyme in its solid-state after spray-drying, however ALDHTt-508 shows major structural recomposition owing to peak shift and broadening (Fig. 4B).

Distortion of the helical conformation continues to increase after 12 weeks of storage. This phenomenon is noted for both proteins, however without the molecular lock, increases in α-helix distortion are four times higher than for the protein with the molecular lock (Table S4 and Fig. 5, ESI†). Loss of native helices is apparent before rehydration in the shift and broadening of the 1655 cm^{-1} peak in the ss-FTIR data in Fig. 4B. Samples of ALDH*Tt*-508 also showed a loss of intensity of β-sheet peaks located in the 1660–1690 cm^{-1} region and at 1618 cm^{-1}. A new peak at ~1682 cm^{-1} forms after storage of both ALDH*Tt*-508 powders for 12 weeks corresponding to β-turns. Both changes are reflected in rehydrated samples in circular dichroism (Table S4, ESI†). ALDH*Tt*-native showed good stability of the α-helices at solid state, with little change in the 1655 cm^{-1} peak between W0 and W12. The spectra however did show minor loss in intensity of the β-sheet peaks at 1630 cm^{-1} and 1638 cm^{-1}. ALDH*Tt*-native shows different changes in conformation in response to SD and storage stresses than ALDH*Tt*-508. The native protein shows lower rates of disordered structures, as well as increases in anti-parallel β-sheets. In an effort to link the role of aldehyde dehydrogenases to amyloid neurodegenerative diseases, other native ALDH proteins with similar quaternary folding have been proven to form amyloid fibrils in the presence of electrical, oxidative and heat stress.[38–40] It is likely therefore that the native ALDH*Tt* protein also tends to the formation of β-sheet dominant amyloid fibrils as aggregates in response to stress present in spray drying. ALDH*Tt*-508, as a mutant and structurally unstable form, is more likely to form non-specific, large order aggregates with no β-sheet formation under SD and storage stress, as corroborated by the CD, FTIR, SE-HPLC and turbidimetry data.

4. Conclusions

This work provides an in-depth evaluation of the effect of a distinct structural feature on the protein's spray drying and solid-state stability. The Box–Behnken DoE employed for the spray drying of ALDH*Tt* showed that the protein can be dried without excipients with >80% residual enzymatic activity, residual moisture content (RM%) of 6.4% and median particle size of 7.84 ± 0.41 μm. The DoE was also applied to a mutant of ALDH*Tt*, which was truncated by 22 amino acids at the C-terminus, losing a 'molecular lock' which contributed to the protein's thermal and oligomeric stability. No changes could be discerned in the properties of both proteins after spray drying, meaning that the mutation did not affect morphology, size, or residual moisture content. The C-terminal extension was found to protect the ALDH*Tt* protein against stresses during the spray drying (SD) process, and consequently reduce storage-related aggregation. Although this 'molecular lock' did not slow down the rate of aggregation during storage, initial stabilisation during the process reduces the volume of misfolded proteins available to form aggregates over time. Additionally, we show that the protein with and without the 'molecular lock' suffered different conformational changes in response to stress. These results show that the SD stability of proteins can be modified by a structural modification or mutation without changing particle properties. This is significant as excipients used in biopharmaceutical formulations are no longer considered 'inert substances' and, particularly need to be minimised in the formulation of inhalables. Further exploration into computationally-directed modelling of terminal extensions in protein would be beneficial for exploiting this adaptation. The C-terminal extension has been previously explored for oligomeric stability in other proteins, however its application has not been discerned until this work.

Author contributions

Wiktoria Brytan: conceptualisation, investigation, writing, project administration. Tewfik Soulimane: supervision, – review & editing, funding acquisition. Luis Padrela: conceptualization, review & editing, supervision, project administration, funding acquisition.

Data availability

The data supporting this article have been included as part of the ESI.†

© 2025 The Author(s). Published by the Royal Society of Chemistry

Open Access Article. Published on 19 December 2024. Downloaded on 5/22/2026 1:24:05 PM. This article is licensed under a Creative Commons Attribution-NonCommercial 3.0 Unported Licence.

Conflicts of interest

There are no conflicts to declare.

Acknowledgements

We thank and acknowledge the Chemical Sciences Department (University of Limerick) for funding and supporting this work. L. Padrela also acknowledges Science Foundation Ireland (SFI) for supporting the work undertaken at the SSPC Research Centre (Phase II grant 12/RC/2775_P2).

References

1 J. M. Slocik, P. B. Dennis, Z. Kuang, A. Pelton and R. R. Naik, Creation of stable water-free antibody based protein liquids, *Commun. Mater.*, 2021, **2**, 118, DOI: **10.1038/s43246-021-00222-2**.

2 M. R. Donthi, A. Butreddy, R. N. Saha, P. Kesharwani and S. K. Dubey, Leveraging spray drying technique for advancing biologic product development–A mini review, *Health Sci. Rev.*, 2024, **10**, 100142, DOI: **10.1016/j.hsr.2023.100142**.

3 J. Li, M. E. Krause, X. Chen, Y. Cheng, W. Dai, J. J. Hill, M. Huang, S. Jordan, D. LaCasse, L. Narhi, E. Shalaev, I. C. Shieh, J. C. Thomas, R. Tu, S. Zheng and L. Zhu, Interfacial Stress in the Development of Biologics: Fundamental Understanding, Current Practice, and Future Perspective, *AAPS J.*, 2019, **21**, 44, DOI: **10.1208/s12248-019-0312-3**.

4 M. Mumenthaler, C. C. Hsu and R. Pearlman, Feasibility study on spray-drying protein pharmaceuticals: recombinant human growth hormone and tissue-type plasminogen activator, *Pharm. Res.*, 1994, **11**, 12–20, DOI: **10.1023/a:1018929224005**.

5 Y.-F. Maa, P.-A. T. Nguyen and S. W. Hsu, Spray-Drying of Air–Liquid Interface Sensitive Recombinant Human Growth Hormone, *J. Pharm. Sci.*, 1998, **87**, 152–159, DOI: **10.1021/js970308x**.

6 K. Ståhl, M. Claesson, P. Lilliehorn, H. Lindén and K. Bäckström, The effect of process variables on the degradation and physical properties of spray dried insulin intended for inhalation, *Int. J. Pharm.*, 2002, **233**, 227–237, DOI: **10.1016/S0378-5173(01)00945-0**.

7 B. A. M. Amdadul Haque, Drying and denaturation of proteins in Spray Drying Process, in *Handbook of Industrial Drying*, ed. A. S. Mujumdar, CRC Press, 2014, pp. 14.9780429169762.

8 P. Boonyai, B. Bhandari and T. Howes, Stickiness measurement techniques for food powders: a review, *Powder Technol.*, 2004, **145**, 34–46, DOI: **10.1016/j.powtec.2004.04.039**.

9 W. Brytan and L. Padrela, Structural modifications for the conversion of proteins and peptides into stable dried powder formulations: a review, *J. Drug Delivery Sci. Technol.*, 2023, **89**, 104992, DOI: **10.1016/j.jddst.2023.104992**.

10 L. Chen, J.-L. Zhang, Q.-C. Zheng, W.-T. Chu, Q. Xue, H.-X. Zhang and C.-C. Sun, Influence of C-terminal tail deletion on structure and stability of hyperthermophile Sulfolobus tokodaii RNase HI, *J. Mol. Model.*, 2013, **19**, 2647–2656, DOI: **10.1007/s00894-013-1816-x**.

11 M. E. Than, P. Hof, R. Huber, G. P. Bourenkov, H. D. Bartunik, G. Buse and T. Soulimane, Thermus thermophilus cytochrome-c552: a new highly thermostable cytochrome-*c* structure obtained by MAD phasing 11Edited by K. Nagai, *J. Mol. Biol.*, 1997, **271**, 629–644, DOI: **10.1006/jmbi.1997.1181**.

12 S. Wang, Y. B. Yan and Z. Y. Dong, Contributions of the C-terminal helix to the structural stability of a hyperthermophilic Fe-superoxide dismutase (TcSOD), *Int. J. Mol. Sci.*, 2009, **10**, 5498–5512, DOI: **10.3390/ijms10125498**.

13 D. L. Klein, S. Radestock and H. Gohlke, Analyzing protein rigidity for understanding and improving thermal adaptation, *Thermostable Proteins: Structural Stability and Design*, 2016, pp. 47–65, **https://www.scopus.com/inward/record.uri?eid=2-s2.0-84860835970&partnerID=40&md5=49ecc23559df2abdb3b63db26de4cb74**.

14 M. Radzi Noor and T. Soulimane, Bioenergetics at extreme temperature: thermus thermophilus ba3- and caa3-type cytochrome *c* oxidases, *Biochim. Biophys. Acta, Bioenerg.*, 2012, **1817**, 638–649, DOI: **10.1016/j.bbabio.2011.08.004**.

15 K. Hayes, M. Noor, A. Djeghader, P. Armshaw, T. Pembroke, S. Tofail and T. Soulimane, The quaternary structure of Thermus thermophilus aldehyde dehydrogenase is stabilized by an evolutionary distinct C-terminal arm extension, *Sci. Rep.*, 2018, **8**, 13327, DOI: **10.1038/s41598-018-31724-8**.

16 W. Brytan, K. Shortall, F. Duarte, T. Soulimane and L. Padrela, Contribution of a C-Terminal Extension to the Substrate Affinity and Oligomeric Stability of Aldehyde Dehydrogenase from Thermus thermophilus HB27, *Biochemistry*, 2024, **63**(9), 1075–1088, DOI: **10.1021/acs.biochem.3c00698**.

17 M. Zanoni, S. Bravaccini, F. Fabbri and C. Arienti, Emerging Roles of Aldehyde Dehydrogenase Isoforms in Anti-cancer Therapy Resistance, *Front. Med.*, 2022, **9**, 795762, DOI: **10.3389/fmed.2022.795762**.

18 K. Shortall, S. Arshi, S. Bendl, X. Xiao, S. Belochapkine, D. Demurtas, T. Soulimane and E. Magner, Coupled immobilized bi-enzymatic flow reactor employing cofactor regeneration of NAD+ using a thermophilic aldehyde dehydrogenase and lactate dehydrogenase, *Green Chem.*, 2023, **25**, 4553–4564, DOI: **10.1039/D3GC01536J**.

19 G. Han, M. R. Webb and A. L. Waterhouse, Acetaldehyde reactions during wine bottle storage, *Food Chem.*, 2019, **290**, 208–215, DOI: **10.1016/j.foodchem.2019.03.137**.

20 F. Rigoldi, S. Donini, A. Redaelli, E. Parisini and A. Gautieri, Review: engineering of thermostable enzymes for industrial applications, *APL Bioenerg.*, 2018, **2**, 011501, DOI: **10.1063/1.4997367**.

21 J. T. Pinto, E. Faulhammer, J. Dieplinger, M. Dekner, C. Makert, M. Nieder and A. Paudel, Progress in spray-drying of protein pharmaceuticals: literature analysis of trends in formulation and process attributes, *Drying Technol.*, 2021, **39**, 1415–1446, DOI: **10.1080/07373937.2021.1903032**.

© 2025 The Author(s). Published by the Royal Society of Chemistry

Open Access Article. Published on 19 December 2024. Downloaded on 5/22/2026 1:24:05 PM. This article is licensed under a Creative Commons Attribution-NonCommercial 3.0 Unported Licence.

22 A. Ziaee, A. B. Albadarin, L. Padrela, T. Femmer, E. O'Reilly and G. Walker, Spray drying of pharmaceuticals and biopharmaceuticals: critical parameters and experimental process optimization approaches, *Eur. J. Pharm. Sci.*, 2019, **127**, 300–318, DOI: **10.1016/j.ejps.2018.10.026**.

23 K. A. Connors, The Karl Fischer Titration of Water, *Drug Dev. Ind. Pharm.*, 1988, **14**, 1891–1903, DOI: **10.3109/03639048809151996**.

24 P. L. Poole and J. L. Finney, Hydration-induced conformational and flexibility changes in lysozyme at low water content, *Int. J. Biol. Macromol.*, 1983, **5**, 308–310, DOI: **10.1016/0141-8130(83)90047-8**.

25 A. P. S. Brogan, G. Siligardi, R. Hussain, A. W. Perriman and S. Mann, Hyper-thermal stability and unprecedented refolding of solvent-free liquid myoglobin, *Chem. Sci.*, 2012, **3**, 1839–1846, DOI: **10.1039/C2SC20143G**.

26 M. Bowen, R. Turok and Y. F. Maa, Spray Drying of Monoclonal Antibodies: Investigating Powder-Based Biologic Drug Substance Bulk Storage, *Drying Technol.*, 2013, **31**, 1441–1450, DOI: **10.1080/07373937.2013.796968**.

27 P. T. Mah, P. O'Connell, S. Focaroli, R. Lundy, T. F. O'Mahony, J. E. Hastedt, I. Gitlin, S. Oscarson, J. V. Fahy and A. M. Healy, The use of hydrophobic amino acids in protecting spray dried trehalose formulations against moisture-induced changes, *Eur. J. Pharm. Biopharm.*, 2019, **144**, 139–153, DOI: **10.1016/j.ejpb.2019.09.014**.

28 S. Ohtake, Y. Kita and T. Arakawa, Interactions of formulation excipients with proteins in solution and in the dried state, *Adv. Drug Delivery Rev.*, 2011, **63**, 1053–1073, DOI: **10.1016/j.addr.2011.06.011**.

29 K. Dill and S. Bromberg, Molecular driving forces: statistical thermodynamics in biology, chemistry, physics, and nanoscience, *Garland Sci.*, 2010, 0203809076.

30 R. Vehring, Pharmaceutical Particle Engineering via Spray Drying, *Pharm. Res.*, 2008, **25**, 999–1022, DOI: **10.1007/s11095-007-9475-1**.

31 S. Marciano, D. Dey, D. Listov, S. J. Fleishman, A. Sonn-Segev, H. Mertens, F. Busch, Y. Kim, S. R. Harvey, V. H. Wysocki and G. Schreiber, Protein quaternary structures in solution are a mixture of multiple forms, *Chem. Sci.*, 2022, **13**, 11680–11695, DOI: **10.1039/d2sc02794a**.

32 N. Grasmeijer, V. Tiraboschi, H. J. Woerdenbag, H. W. Frijlink and W. L. J. Hinrichs, Identifying critical process steps to protein stability during spray drying using a vibrating mesh or a two-fluid nozzle, *Eur. J. Pharm. Sci.*, 2019, **128**, 152–157, DOI: **10.1016/j.ejps.2018.11.027**.

33 M. Batens, T. A. Shmool, J. Massant, J. A. Zeitler and G. Van den Mooter, Advancing predictions of protein stability in the solid state, *Phys. Chem. Chem. Phys.*, 2020, **22**, 17247–17254, DOI: **10.1039/D0CP00341G**.

34 L. Chang and M. J. Pikal, Mechanisms of protein stabilization in the solid state, *J. Pharm. Sci.*, 2009, **98**, 2886–2908, DOI: **10.1002/jps.21825**.

35 M. Bernhofer, C. Dallago, T. Karl, V. Satagopam, M. Heinzinger, M. Littmann, T. Olenyi, J. Qiu, K. Schütze, G. Yachdav, H. Ashkenazy, N. Ben-Tal, Y. Bromberg, T. Goldberg, L. Kajan, S. O'Donoghue, C. Sander, A. Schafferhans, A. Schlessinger, G. Vriend, M. Mirdita, P. Gawron, W. Gu, Y. Jarosz, C. Trefois, M. Steinegger, R. Schneider and B. Rost, PredictProtein – Predicting Protein Structure and Function for 29 Years, *Nucleic Acids Res.*, 2021, **49**, W535–W540, DOI: **10.1093/nar/gkab354**.

36 R. Sajó, O. Tőke, I. Hajdú, H. Jankovics, A. Micsonai, J. Dobó, J. Kardos and F. Vonderviszt, Structural plasticity of the Salmonella FliS flagellar export chaperone, *FEBS Lett.*, 2016, **590**, 1103–1113, DOI: **10.1002/1873-3468.12149**.

37 A. A. H. Zanjani, N. P. Reynolds, A. Zhang, T. Schilling, R. Mezzenga and J. T. Berryman, Amyloid Evolution: Antiparallel Replaced by Parallel, *Biophys. J.*, 2020, **118**, 2526–2536, DOI: **10.1016/j.bpj.2020.03.023**.

38 L. M. Cortez, C. L. Ávila, C. M. Torres Bugeau, R. N. Farías, R. D. Morero and R. N. Chehín, Glyceraldehyde-3-phosphate dehydrogenase tetramer dissociation and amyloid fibril formation induced by negatively charged membranes, *FEBS Lett.*, 2010, **584**, 625–630, DOI: **10.1016/j.febslet.2009.12.012**.

39 H. Nakajima, W. Amano, T. Kubo, A. Fukuhara, H. Ihara, Y.-T. Azuma, H. Tajima, T. Inui, A. Sawa and T. Takeuchi, Glyceraldehyde-3-phosphate Dehydrogenase Aggregate Formation Participates in Oxidative Stress-induced Cell Death, *J. Biol. Chem.*, 2009, **284**, 34331–34341, DOI: **10.1074/jbc.M109.027698**.

40 G. Garza-Ramos, C. Mújica-Jiménez and R. A. Muñoz-Clares, Potassium and Ionic Strength Effects on the Conformational and Thermal Stability of Two Aldehyde Dehydrogenases Reveal Structural and Functional Roles of K + -Binding Sites, *PLoS One*, 2013, **8**, e54899, DOI: **10.1371/journal.pone.0054899**.

© 2025 The Author(s). Published by the Royal Society of Chemistry